Chemical Engineering Journal 99 (2004) 5–14

Chemical Engineering Journal

www.elsevier.com/locate/cej

Axial flow structure at the varying superficial gas velocity in a downer reactor

Rensheng Deng, Huie Liu, Fei Wei*, Yong Jin

Fluidization Laboratory of Tsinghua University (FLOTU), Department of Chemical Engineering, Tsinghua University, Beijing 100084, PR China

Received 26 October 2002; accepted 8 August 2003

Abstract

A one-dimensional model based on the conservation equations of mass and momentum together with the reaction kinetics is developed to predict the axial flow structure in a downer reactor at the varying superficial gas velocity (SGV). The predictions show that, compared to the case of constant SGV, the varying SGV can change the axial flow behaviors for both gas and particle phases and new features appear in the axial distribution of flow parameters such as the gas velocity, particle velocity, solids concentration, pressure and pressure gradient. It is revealed by the simulation that the influences of the varying SGV on the products yield are significant and must be considered in the commercial application of the downer reactor.

Keywords: Downer reactor; Axial flow structure; Gas velocity

1. Introduction

Downer reactor is a novel circulating fluidized bed (CFB) which draws the attention of many researchers in recent years. The hydrodynamics study [1–6] shows that the radial distribution of flow parameters such as particle velocity, gas velocity and solids concentration in the downer is more uniform than in the riser, and it was also stated that the radial flow structure does not result in severe radial non-uniformity even in a fast reaction like fluid catalytic cracking (FCC) [7]. Therefore, the importance of the axial flow structure becomes very significant.

The axial behaviors in downer reactors have been investigated for long [8–14]. During these experiments, the superficial gas velocity (SGV) remains unchanged along the reactor length. This is obviously not the actual situation in commercial reactors where the SGV often varies with the changes of molecules, pressure, temperature or cross-section area at different axial positions. For example, the SGV at the inlet of an FCC plant is typically 5–7 m/s while at the exit it increases to 18–19 m/s due to the increase in molecule number. Such significant changes in gas velocity are sure to characterize the axial behaviors and further influence the distribution of products. Thus, the study on the hydrodynamics at a varying SGV is very important for the application of downer reactor, while few results have been reported in literature on this topic.

In this work, a one-dimensional model is developed to investigate the axial flow structure in a downer reactor by coupling the conservation equations of mass and momentum with the kinetics of model reactions. Due to the different reaction schemes adopted, various distribution forms of SGV along the reactor length are introduced and examined in more detail.

2. Model description

As shown in Fig. 1, pure reactant **A** and the solid catalyst are introduced into the downer reactor from the top, and the mixture of unconverted **A**, product **B** and the used catalyst are discharged from the bottom. If the gas–solids flow is considered steady, the following equation is satisfied for any variable Ω:

$$\frac{\partial \Omega}{\partial t} = 0 \tag{1}$$

Abbreviations: CFB, circulating fluidized bed; CVZ, constant velocity zone; DZ, decreasing zone; FAZ, first accelerating zone; FCC, fluid catalytic cracking; SAZ, second accelerating zone; SGV, superficial gas velocity; TAZ, third accelerating zone

* Corresponding author. Tel.: +86-10-62785464; fax: +86-10-62772051.
E-mail address: wf-dce@mail.tsinghua.edu.cn (F. Wei).

1385-8947/$ – see front matter © 2003 Elsevier B.V. All rights reserved.
doi:10.1016/j.cej.2003.08.024

Nomenclature

A_0	reactor cross-section area (m^2)
C_A	concentration of **A** (mol/m^3)
C_d	drag force coefficient between particles and gas (–)
C_{ds}	drag force coefficient between a single particle and gas (–)
d_p	particle diameter (m)
D	reactor diameter (m)
F_D	drag force (N/m^3)
F_f	friction between fluid (particle) and wall (N/m^3)
Fr	Froude number ($=u_g/\sqrt{gd_p}$)
g	gravitational acceleration ($9.8\,m/s^2$)
G	flux ($kg/m^2\,s$)
k_A	reaction rate constant (kmol/(kgcat s) for $n = 0$, m^3/(kgcat s) for $n = 1$, m^6/(kmol kgcat s) for $n = 2$)
L(I)	length of the first accelerating zone (m)
m	phase ratio (–)
M_A	molecular weight of product **A** (kg/kmol)
M_B	molecular weight of product **B** (kg/kmol)
n	reaction order (–)
P	pressure (Pa)
r_A	reaction rate (kmol/(kgcat s))
R	universal gas constant ($8.314\,J/(mol\,K)$)
t	time (s)
T	temperature (K)
U_g	superficial gas velocity (m/s)
V	velocity (m/s)
W_T	mass flow rate of gas (kg/s)
x	length from the reactor inlet (m)
y_A	weight fraction of substance **A** in the mixture (–)

Subscripts

g	gas
p	particle
0	initial value

Greek letters

ε	voidage (–)
λ_f	total friction coefficient between gas-particle and wall (–)
λ_g	friction coefficient between gas and wall (–)
ρ	density (kg/m^3)

The mass conservation equations then can be written as the following by ignoring the small non-uniformity along radial dimension:

$$\text{Gas phase}: \quad \frac{\partial(\varepsilon\rho_g V_g)}{\partial x} = 0 \tag{2}$$

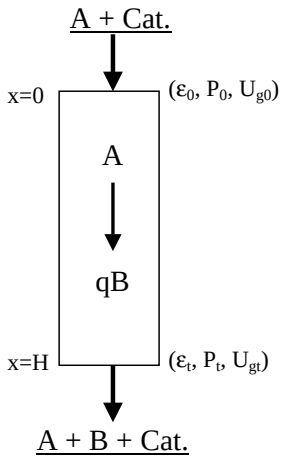

Fig. 1. A downer reactor with the chemical reaction happening inside.

$$\text{Solid phase}: \quad \frac{\partial((1-\varepsilon)\rho_P V_P)}{\partial x} = 0 \tag{3}$$

And the corresponding momentum conservation equations are

$$\text{Gas phase}: \quad \frac{\partial(\varepsilon\rho_g V_g^2)}{\partial x} = -\frac{\partial P}{\partial x} \mp F_D - F_{fg} + \varepsilon\rho_g g \tag{4}$$

$$\text{Solid phase}: \quad \frac{\partial[(1-\varepsilon)\rho_P V_P^2]}{\partial x} = \pm F_D - F_{fp} + (1-\varepsilon)(\rho_p - \rho_g)g \tag{5}$$

Note that the upper sign denotes the variable in the first accelerating zone (FAZ) and the lower denotes that in the second accelerating zone (SAZ) when "$\mp$" or "$\pm$" appears.

For the given gas flux and solids flux, the following equations can be obtained from (2) and (3):

$$G_g = \varepsilon\rho_g V_g = \text{const.} \tag{6}$$

$$G_s = (1-\varepsilon)\rho_p V_p = \text{const.} \tag{7}$$

By substituting the above into (4) and (5) we get

$$G_g\frac{\partial V_g}{\partial x} = -\frac{\partial p}{\partial x} \pm F_D - F_{fg} + \varepsilon\rho_g g \tag{8}$$

$$G_s\frac{\partial V_p}{\partial x} = \pm F_D - F_{fp} + (1-\varepsilon)(\rho_p - \rho_g)g \tag{9}$$

where the drag force and the friction can be calculated by the following (Ref. [15]):

$$F_D = \frac{3}{4}\frac{C_d}{d_p}(1-\varepsilon)\rho_g(V_g - V_p)^2 \tag{10}$$

$$F_{fg} = \frac{1}{2}\lambda_g\frac{\rho_g V_g^2}{D} \tag{11}$$

$$F_{fp} = \frac{1}{2}(\lambda_f - \lambda_g)\frac{\rho_g V_g^2}{D} \tag{12}$$

The SGV and the gas density can be expressed as

$$U_g = V_g \varepsilon \tag{13}$$

$$\rho_g = \frac{G_g}{\varepsilon V_g} = \frac{G_g}{U_g} \tag{14}$$

Substitute Eqs. (10)–(14) into (9), and define

$$\frac{G_g}{G_s} = \frac{1}{m} \tag{15}$$

$$\frac{G_s}{\rho_p U_g} = (1-\varepsilon)^* \tag{16}$$

Finally we get

$$\frac{d\varepsilon}{dx} = \frac{1}{m(1-\varepsilon)^*}\left[\pm\frac{3C_d}{4d_p}(1-\varepsilon)^3\left(\frac{1}{\varepsilon} - \frac{(1-\varepsilon)^*}{1-\varepsilon}\right)^2 - \frac{\lambda_f - \lambda_g}{2D}\frac{(1-\varepsilon)^2}{\varepsilon^2} + \frac{g}{U_g^2}\left(\frac{m}{(1-\varepsilon)^*} - 1\right)(1-\varepsilon)^3\right] \tag{17}$$

The boundary condition is given by

$$x = 0, \qquad \varepsilon = \varepsilon_0 \tag{18}$$

The drag force coefficient is calculated from the correlation suggested by Jin et al. [16]:

$$\frac{C_d}{C_{ds}} = \frac{14.1(1 + 2.78/m)}{Fr} \tag{19}$$

According to Eq. (8), the pressure gradient along the reactor length can be determined by

$$\frac{dP}{dx} = \mp F_D - F_{fg} + \varepsilon\rho_g g - G_g\frac{d(U_g/\varepsilon)}{dx} \tag{20}$$

together with the boundary condition:

$$x = 0, \qquad P = P_0 \tag{21}$$

Suppose the irreversible model reaction with the action of solid catalysts in the following form:

$$A \rightarrow qB \tag{22}$$

where both **A** and **B** are in gas state. For $q < 1$, $q = 1$ and $q > 1$, the above equation denotes a reaction during which the molecule number reduces, conserves and increases, respectively.

If the reaction order to **A** is n, then the reaction rate can be expressed as

$$-r_A = k_A C_A^n \tag{23}$$

And the mass balance in the infinitesimal of the reactor gives

$$\frac{dy_A}{dx} = r_A\rho_P(1-\varepsilon)A_0\frac{M_A}{W_T} \tag{24}$$

Finally the varying rate of SGV can be obtained as the following:

For zero-order reaction ($n = 0$):

$$\frac{dU_g}{dx} = \frac{1}{P}\left[(q-1)k_A\rho_P(1-\varepsilon)RT - U_g\frac{dP}{dx}\right] \tag{25a}$$

For first-order reaction ($n = 1$):

$$\frac{dU_g}{dx} = \frac{1}{P}\left[k_A\rho_P(1-\varepsilon)P\left(\frac{W_T RT}{PU_g A_0 M_B} - 1\right) - U_g\frac{dP}{dx}\right] \tag{25b}$$

For second-order reaction ($n = 2$):

$$\frac{dU_g}{dx} = \frac{1}{P}\left[k_A\rho_P(1-\varepsilon)\frac{P^2}{RT}\frac{(W_T RT/PU_g A_0 M_B - 1)^2}{q-1} - U_g\frac{dP}{dx}\right] \tag{25c}$$

and the boundary condition is

$$x = 0, \qquad U_g = U_{g_0} \tag{26}$$

Eqs. (17), (20) and (25) constitute a set of ordinary differential equations in the variables of ε, P and U_g, which can be closed by supplying the boundary conditions of (18), (21) and (26). A fourth-order Runge–Kutta method is applied to solve the problem numerically. Note that the radial non-uniformity in flow structure and particle clustering are not taken into consideration in this model.

It should be mentioned that the variation in temperature along the reactor length also influences the SGV distribution, and it is applicable to couple the energy conservation equation into the present analysis to obtain the understanding of such effects. However, with regard to the purpose of this work, an isothermal assumption throughout the whole reactor is adopted here in order to simplify the problem and concentrate on the study of the axial flow structure. For the same reason, only the initial value problems are tested, although the boundary value problems are also accepted by this model.

3. Results and discussion

3.1. Comparison between the varying and constant SGV cases

When q is set at 1.0, the molecule number is identical before and after the reaction. Although the SGV can be influenced by the pressure variation according to Eq. (25), it almost keeps unchanged at different axial locations because the pressure gradient is very small in comparison with the pressure. This is the situation under the cold-model experimental conditions and is referred to as *the constant SGV*

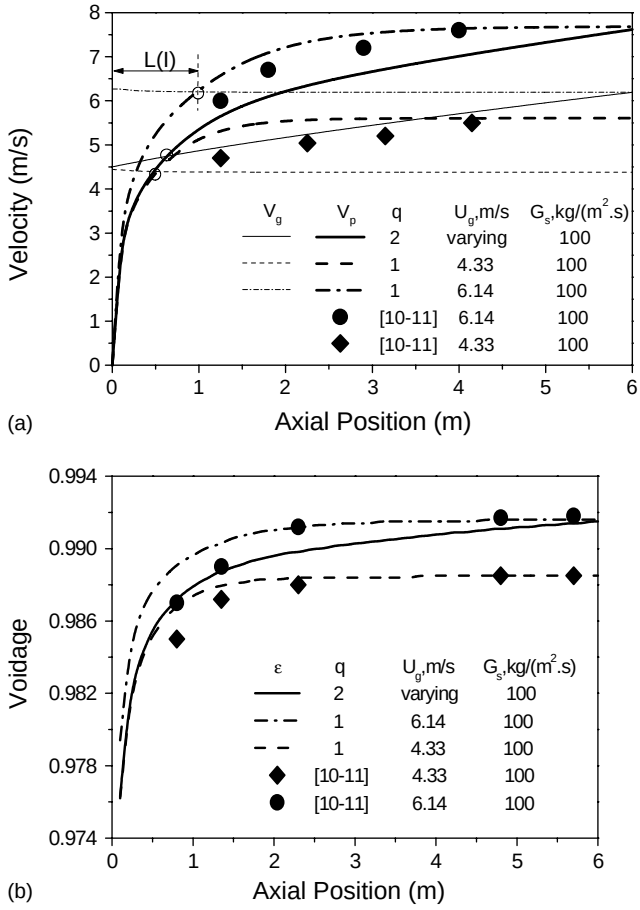

Fig. 2. (a) Axial distribution of gas velocity and particle velocity in the downer at the constant and varying SGV; (b) axial distribution of voidage in the downer at the constant and varying SGV.

case. If q is not equal to 1.0, however, the SGV will increase (decrease) as a result of the increase (decrease) in molecule number along the reactor, which is called *the varying SGV case*.

The model particle in the simulation is the FCC catalyst used by Qi et al. [10,11], with the density of 1545 kg/m^3 and the diameter of 59 μm. The model reactor is 140 mm in inner diameter and 6 m in height with air as the fluidized gas. The temperature is set at 20 °C and solids reflux used is 100 kg/(m^2 s), and the voidage (ε_0) at the inlet is 0.6. The downer used by Qi et al. [10,11] is 5.8 m in height, while other parameters such as the reactor diameter and operating conditions are the same as adopted in this simulation.

The axial distribution of gas and particle velocities at constant SGV values of 4.33 and 6.14 m/s is shown in Fig. 2(a). In these two cases, the corresponding initial values of pressure are set at 150 and 1250 Pa above the atmosphere pressure, respectively. It can be seen that the simulation results fit well with the experimental data of Qi et al. [10,11]. After being introduced from the inlet, the particles enter the FAZ in which they are under the joint action of gravity and drag force. The resultant high acceleration leads to a sharp increase of particle velocity until it equals to the gas velocity (denoted by a hollow circle in Fig. 2). After that, the SAZ starts where particles continue to accelerate due to the existence of gravity, but the direction of drag force turns upwards because the particle velocity is higher than the gas velocity. In this case, the drag force becomes a resistance to the particle movement, which grows larger and larger with the increasing particle velocity and finally balances the gravity, indicating the end of the SAZ. In the following constant velocity zone (CVZ), the particle velocity keeps unchanged and a constant difference of velocity exists between the gas and the particle.

Fig. 2(a) also shows the gas and particle velocities along the reactor length for the varying SGV case with a q value of 2.0. The SGV is selected as 4.33 m/s at the inlet and 6.14 m/s at the exit by adopting $n = 0$ and a reaction rate constant of 0.742 kmol/(kgcat s), and the initial pressure is assumed at 800 Pa above the atmosphere pressure. Again, the particles are accelerated by gravity and drag force in the FAZ, and the particle velocity profile is close to the constant SGV case of 4.33 m/s except that the particle velocity catches up with the gas velocity at a longer axial position, i.e. a higher L(I) value (length of the FAZ) is necessary here. However, particle velocity is no more similar as the 4.33 m/s case in the SAZ but tends to approach gradually the case of 6.14 m/s. A significant feature of the varying SGV case is that CVZ disappears, which can be explained by the analysis on force balance. Assuming that a constant particle velocity could be reached, the velocity gap between the gas and particles would reduce because of the continuous increase of the gas velocity. According to Eq. (10), the drag force would decrease and could not balance the gravity any more; as a result the particle velocity would increase continuously, which conflicts with the assumption. It can be seen from Fig. 2(a) that the curve of particle velocity at the varying SGV can be viewed as a certain kind of combination of the two constant cases, although detailed values can only be predicted by the adoption of mathematical model due to the strong influence of nonlinear factors.

In the commercial application of fluidized beds, the solid particles are often used as catalyst, absorbent or heat carrier, and the determination of mean cross-section voidage is always of great value.

It can be seen from Fig. 2(b) that the simulated axial distribution of voidage for the constant SGV case agrees well with the experimental results of Qi et al. [10,11]. According to Eq. (7), the rapid increase of particle velocity results in the sharp increase of voidage in the inlet part, while this tendency gradually slows down and finally a stable voidage is reached in the exit part. On the other hand, the particle velocity at the varying SGV case is close to the 4.33 m/s case in the FAZ and then tends to approach the 6.14 m/s case in the SAZ. Different from the constant SGV case, the voidage continuously increases along the reactor length and no stable value would be attained.

The measurement of pressure distribution is often a useful method to obtain information about catalyst concentration

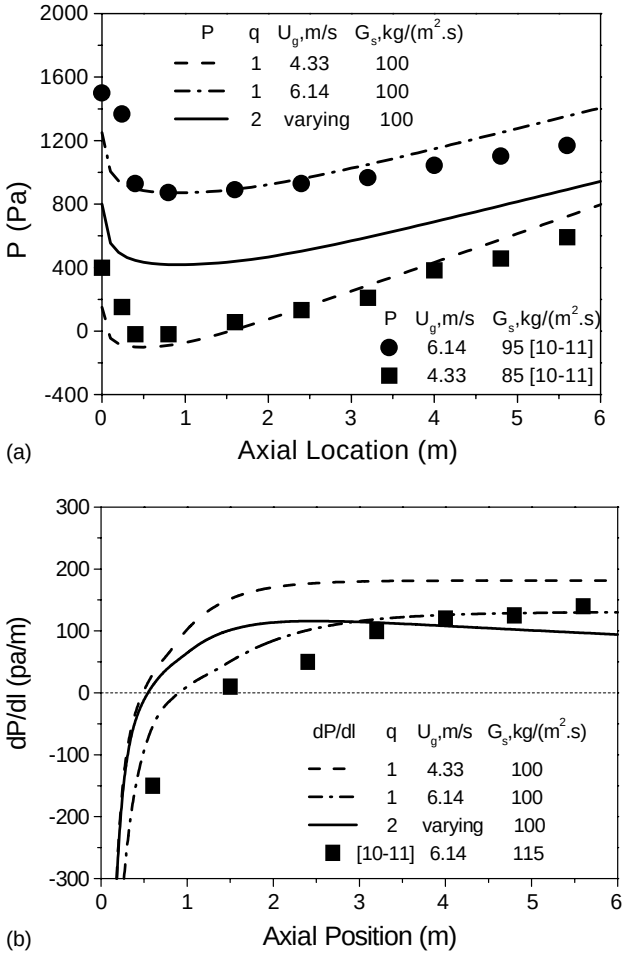

Fig. 3. (a) Axial distribution of pressure in the downer at the constant and varying SGV; (b) axial distribution of pressure gradient in the downer at the constant and varying SGV.

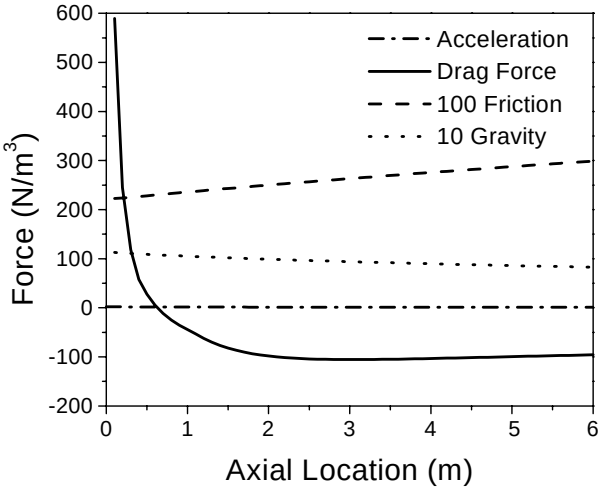

Fig. 4. Distribution of different forces along the reactor length at the varying SGV.

especially for commercial plants operating at high temperature. Fig. 3(a) shows the axial pressure distribution for both the constant and varying SGV cases.

In the FAZ, the loss of gravitational energy during the downflowing of gas–solids cannot meet the needs for solids accelerating and overcoming friction between wall and fluid, therefore the pressure decreases sharply to fill the gap. After entering the SAZ, one part of the gravitational energy is continuously converted to the kinetic energy of particles, another part is used to overcome friction, and the rest is stored as the static pressure of gas, which leads to an increasing pressure along the reactor length. After experiencing the pressure-decreasing and pressure-increasing procedure, the pressure drop of the whole reactor may be positive, negative or zero. Such an analysis is valid for both cases.

As shown in Fig. 3(b), the pressure gradient for the constant SGV case is negative in the FAZ and increases sharply along flow direction. After that, the increase becomes smooth and finally the pressure gradient remains at a constant value. In the varying SGV case, the pressure gradient also follows a sharp-to-smooth increasing period at the beginning, however, it turns to decrease after a maximum is reached. The reason can be obtained by examining the forces acting on the particles, as shown in Fig. 4. The drag force between gas and solids is much larger than the gas–wall friction and the gas gravity, while the gas acceleration is very small. Thus, the value of pressure gradient mainly depends on the drag force according to Eq. (8). Although the velocity difference between gas and particle keeps increasing in the SAZ, the drag force attains a peak and then reduces along the reactor length due to the effects of other items in Eq. (10), for example, the decrease of gas density and solids fraction.

3.2. Effects of G_s and G_g at the varying SGV

Two parameters are of special importance in the CFB operation: feeding rate and solids reflux, which correspond to G_g and G_s in our model. In this part, their effects on the axial flow structure for the varying SGV case are examined with the same conditions as adopted in Section 3.1 except the differences in G_g or G_s.

As shown in Fig. 5(a), the curves of gas velocity versus axial location at different values of G_g are almost parallel. At the same axial position, both the gas velocity and particle velocity increase with the increasing G_g, and a larger L(I) is necessary for a higher value of G_g. This is similar to the constant SGV cases (4.13 and 6.14 m/s) [12]. Moreover, according to Eq. (7), the solids fraction is inversely proportional to the particle velocity given the same solids reflux, thus the voidage increases with the increasing G_g as indicted by Fig. 5(b).

According to Fig. 5(c), a sharp decrease in pressure occurs in the FAZ at all values of G_g while the recovering process is different. For a lower G_g, the location where pressure ceases decreasing and turns to increase is closer to the inlet, and a higher value of pressure is attained at the reactor exit. Thus,

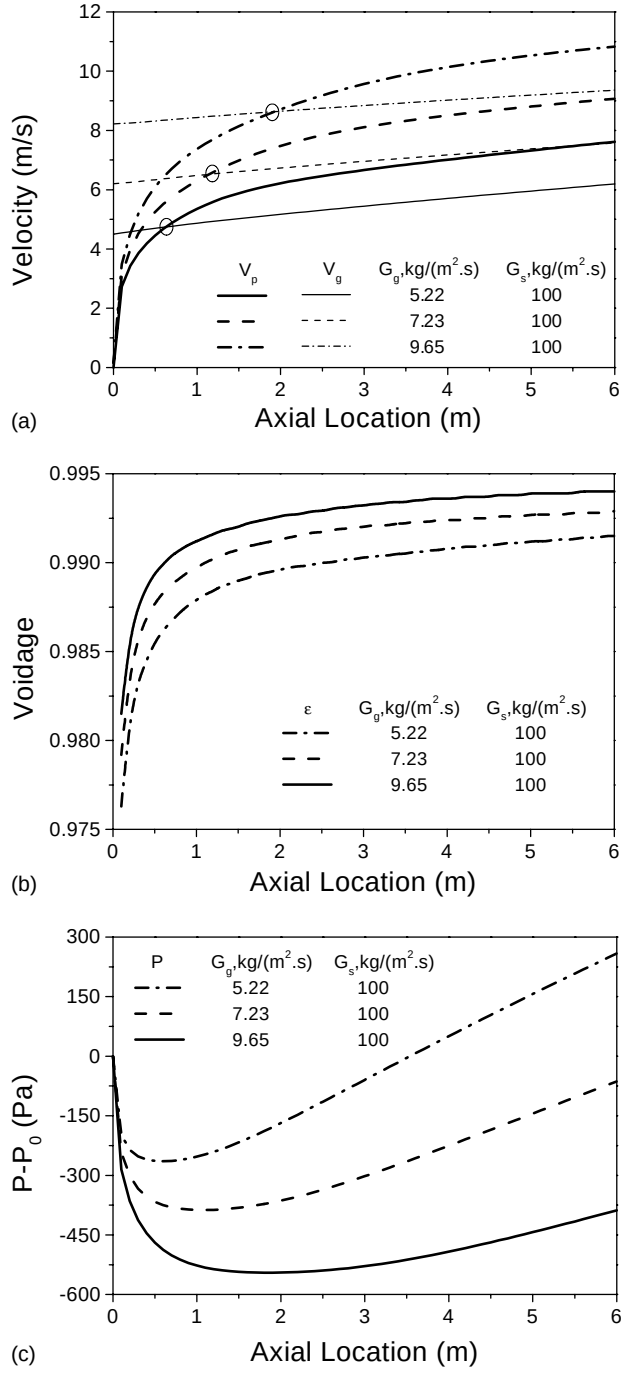

Fig. 5. Comparison of the axial distribution of flow parameters at the varying SGV between different G_g values: (a) gas velocity and particle velocity; (b) voidage; (c) pressure.

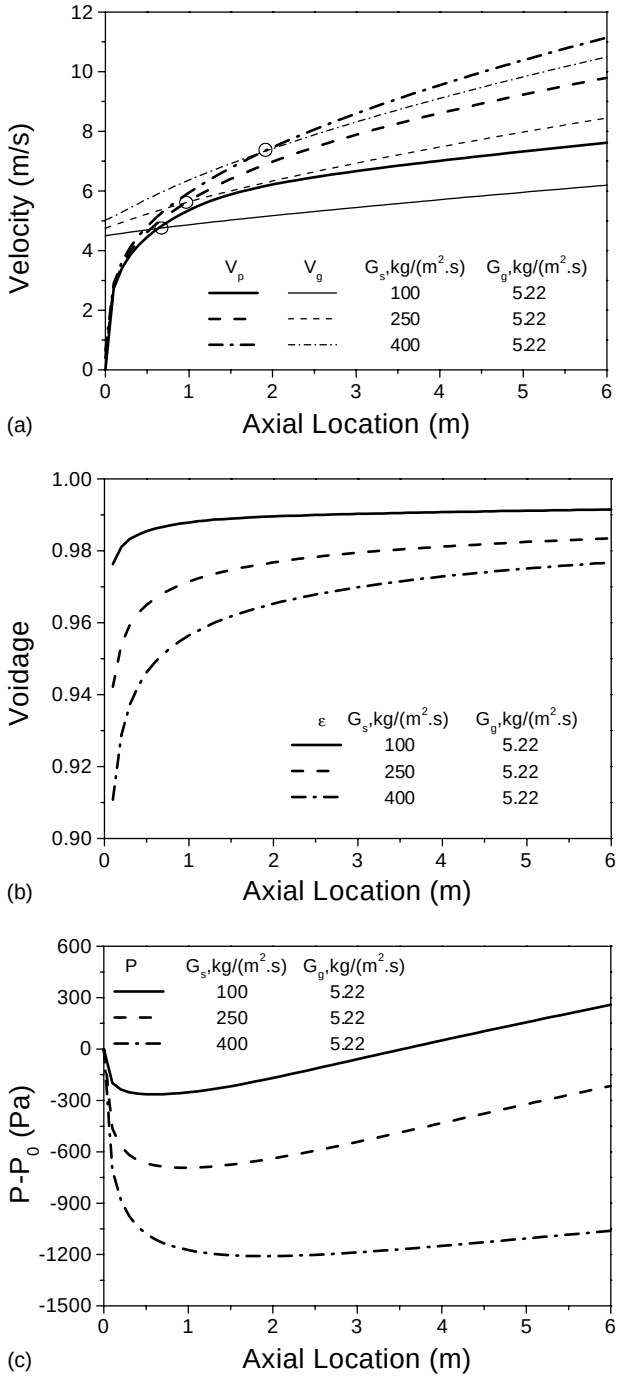

Fig. 6. Comparison of the axial distribution of flow parameters at the varying SGV between different G_s values: (a) gas velocity and particle velocity; (b) voidage; (c) pressure.

small values of G_g (e.g. 5.22 kg/m^2 s) results in a pressure rise in the whole reactor while a pressure drop is obtained at large values of G_g (e.g. 9.65 kg/m^2 s).

Fig. 6(a) shows the axial distribution of velocities at different values of solids reflux. The gas velocity increases sharper along the flow direction when G_s is larger and the particle velocity has the same tendency, which results in a longer L(I) for a higher solid reflux. This is significantly different from the constant SGV case in which the L(I) is influenced little by the variation of G_s [12]. Additionally, the increase of G_s leads to an increase in the phase ratio m, which leads to a decrease in voidage as shown in Fig. 6(b).

The pressure distribution at different values of G_s is shown in Fig. 6(c). At a high solid reflux like 400 kg/m^2 s, the pressure decrease in the FAZ is sharper while the pressure recovery in the SAZ is smoother than at a small solids reflux

like 100 kg/m^2 s, which results in the pressure drop of the whole reactor in the former and the pressure rise in the latter.

3.3. Axial behavior at different q values

The q value represents the change in molecule number during the reaction. Because both the reactant and the product are gas, it denotes the expansion or shrinking in the volume of the system which results in the variation of SGV along the reactor length. The axial behaviors at different q values are examined by adopting the same conditions in Section 3.1 except that the reactor length, initial velocity and reaction rate constant are set at 20 m, 4.0 m/s and 0.87 kmol/(kgcat s), respectively. The axial distribution of velocities is shown in Fig. 7(a) where four cases are considered.

Case (I) is similar to the sample in Section 3.1. Particles are accelerated by both the gravity and the drag force in the FAZ until the particle velocity catches up with the gas velocity. Then in the SAZ the particle velocity is higher than the gas velocity, and the drag force becomes the resistance of particle movement. Due to the absence of CVZ, the particle velocity increases continuously and is always larger than the gas velocity.

In case (II), the increase of SGV along the reactor length is more significant. Similar to case (I), particle velocity is less than gas velocity in the FAZ and after passing the separation point between FAZ and SAZ (denoted by the left hollow circle) it becomes larger than the gas velocity, however this is accompanied by the decrease of particle acceleration due to the direction change of drag force. When the particle acceleration is reduced enough to be lower than the increasing rate of the gas velocity, the gas velocity overtakes the particle velocity at a certain position, which means the end of the SAZ (denoted by the right hollow circle). After that, the direction of the drag force changes again and both the drag force and the gravity accelerate the particles, however the particle acceleration is lower than the increasing rate of gas velocity, which causes the gas velocity to be always higher than the particle velocity. This zone can be called the third accelerating zone (TAZ). It should be mentioned that whether the TAZ appears depends on not only the value of q but also the reactor length.

In case (III), the SGV increases more sharply in the flow direction. Although the particle acceleration is higher than the increasing rate of gas velocity at the beginning of FAZ, it begins to decrease and soon turns to be lower than the increasing rate of gas velocity, which results in the lower particle velocity than the gas velocity during the entire movement and the drag force always serves to accelerate the particles. That is, there is no existence of the SAZ.

Different from the cases above, the SGV in case (IV) decreases gradually along the reactor length. The particle velocity equals to the gas velocity at the end of the FAZ (denoted by the hollow circle). In the SAZ, the particle velocity is higher than the gas velocity, thus the drag force turns upwards and the particle acceleration decreases. The drag force keeps increasing because of the enlarging gap between particle velocity (increasing) and gas velocity (decreasing), finally it balances the gravity and the SAZ is ended, corresponding to the highest particle velocity (denoted by the solid circle). Later then, the decrease of gas velocity leads to the further increase of the drag force and it becomes larger than the gravity, thus the particles are decelerated, indicating the existence of the decelerating zone (DZ). However, the co-gravity movement ensures that the particle velocity is larger than the gas velocity. Even the gas velocity decreases to zero, the particles will flow downwards at the terminal velocity.

The voidage distribution for the four cases above is shown in Fig. 7(b). When q is larger than 1.0, the voidage increases along the reactor length, and a larger q is related to a higher increasing rate. For $q < 1.0$, the voidage increases at first and then decreases, forming a peak at the position corresponding to the maximum of particle velocity in the case (IV) of Fig. 7(a). Note that $q = 1$ represents the constant SGV case mentioned above.

Fig. 7(c) shows that the distribution of pressure along the flow direction differs at different q values. For small q values (e.g. 0.8 and 2.0), the pressure decreases at the beginning and then increases, and a higher increasing rate is obtained by a smaller q. If q is larger than a critical value (such as $q = 5.0$ and 7.0), the pressure decreases all the time along the reactor length and a higher q corresponds to a higher decreasing rate.

It should be mentioned that the various cases above can also be obtained by altering the reaction rate constant k_A. According to Eq. (25), the variation of k_A or q has the similar effects in determining the SGV.

3.4. Axial flow structure at different reaction orders

According to Eq. (25), reactions with different orders have different expressions for SGV. The effects of reaction order n on the axial flow structure are examined by adopting the same conditions in Section 3.1 except the value of k_A which is equal to 0.16 kmol/(kgcat s), 0.16 m^3/(kgcat s) and 0.16 m^6/(kmol kgcat s) for $n = 0$, 1 and 2, respectively.

The axial distribution of gas and particle velocities at different reaction orders is shown in Fig. 8(a). For the zero-order reaction, the gas velocity increases almost linearly but slowly along the reactor length. Differently, the increase in gas velocity is rapid at the beginning and then slows down for the first-order reaction, and such a tendency of sharp-to-smooth increase is more significant for the second-order reaction. The particle velocity rises sharply at the beginning and then tends to be smooth at $n = 0$, while it keeps a high increase rate along the whole reactor length at $n = 1$ and 2. Due to the joint effects of particle velocity

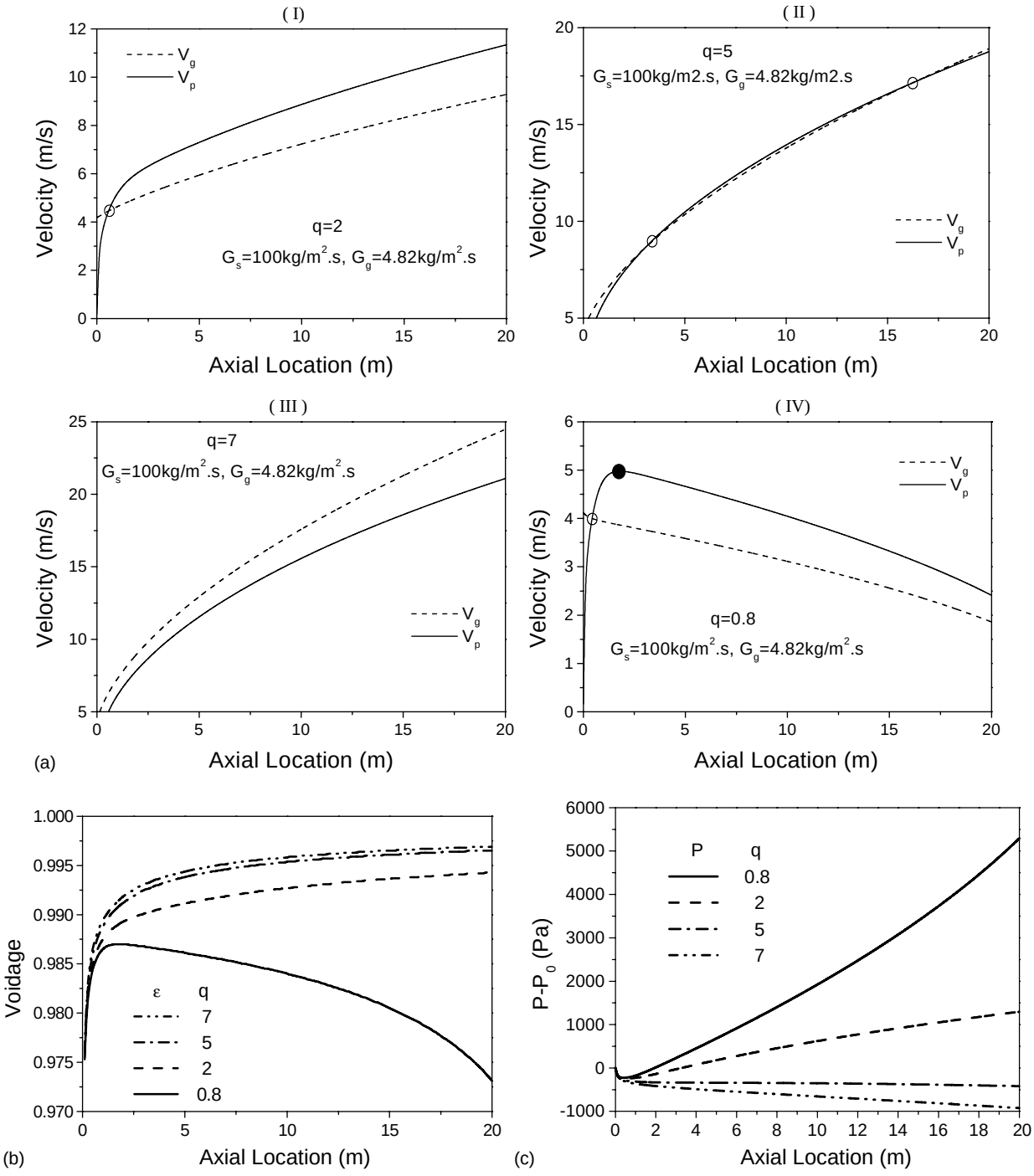

Fig. 7. Comparison of the axial distribution of flow parameters at the varying SGV between different q values: (a) gas velocity and particle velocity; (b) voidage; (c) pressure.

and gas velocity, the L(I) is the shortest at $n = 0$ and the longest at $n = 2$.

Fig. 8(b) shows that the voidage along the flow direction at different values of n. A higher reaction order to the reactant **A** means a higher reaction rate at the same concentration of **A** and causes a higher expansion rate of the system volume, which results in a higher voidage. However, because the expansion index q is same for the three cases, the final voidage obtained after the completion of the chemical reaction will be the same, although a longer reactor is necessary to finish the reaction with a lower reaction order.

The pressure distribution is shown in Fig. 8(c). In all the three cases, the pressure experiences a decreasing and recovering process, while the decreasing is faster and the

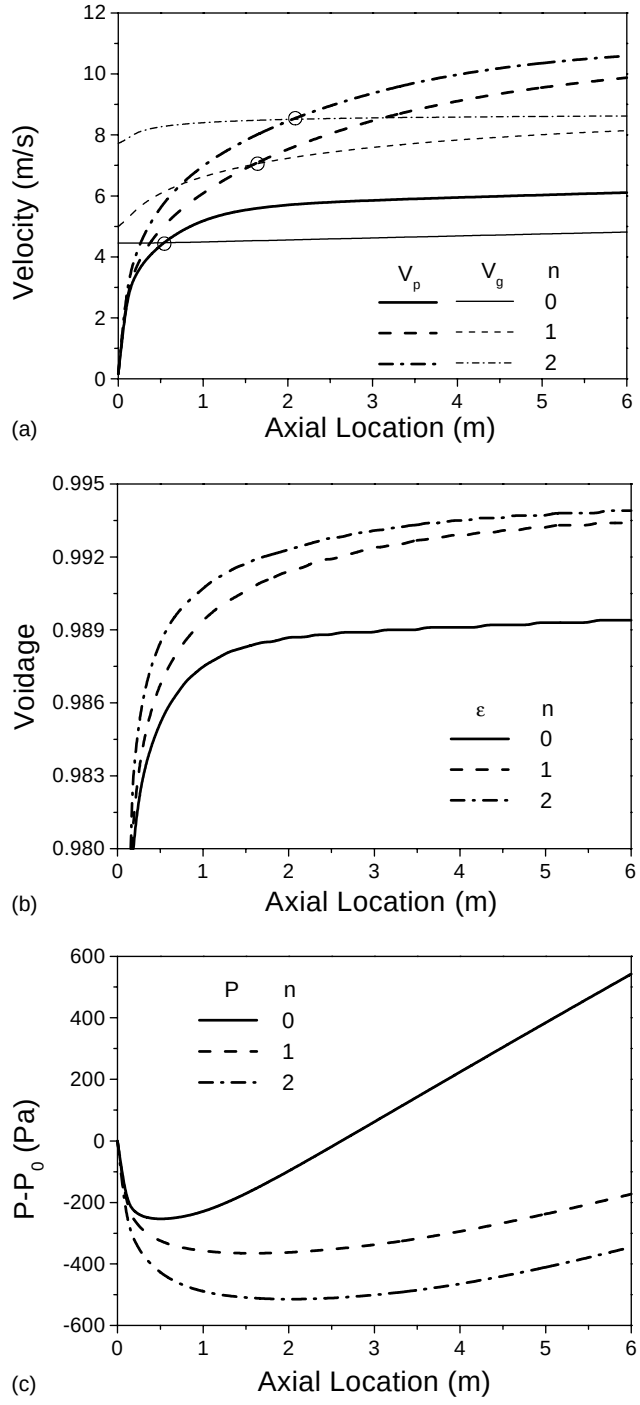

Fig. 8. Comparison of the axial distribution of flow parameters at the varying SGV between different reaction orders: (a) gas velocity and particle velocity; (b) voidage; (c) pressure.

recovering is slower at a higher reaction order. Furthermore, the recovering rate of pressure at $n = 0$ tends to decrease in the rear part of the downer, indicating a decreasing pressure gradient as shown in Fig. 3(b); on the contrary an increasing pressure gradient along the flow direction can be predicted at $n = 1$ and 2 according to the corresponding curve shapes in Fig. 8(c).

3.5. Influences of varying SGV on the product yield

In fact, the varying SGV in the downer not only endues the axial flow structure with new features but also results in characteristic product yields. This attributes to the complex interaction between hydrodynamics and chemical reactions. First, the axial flow structure can directly influence the reaction rate. For example, the gas velocity determines the reaction time, the particle velocity affects the deactivation degree of catalyst, the various solid fractions cause differences in the reaction rate in the control volume, and the pressure can influence the kinetics or thermodynamics of gas phase reactions. Secondly, as shown in Eqs. (17), (20) and (25), the gas velocity, particle velocity, solid fraction and pressure can influence each other and are also dependent on each other. And thirdly, the product distribution will reversely work on the hydrodynamics. Since the volume of the system is related to the gas moles, the variety in the number and type of molecules leads to a varying SGV that shapes the flow structure. All these effects add to the difficulty in predicting the yields of products.

In order to simplify the prediction of product distribution, some approximate methods based on the constant SGV solutions are often used to obtain a rough estimation. Here we examine four means of approximation: (1) adopting the axial flow structure at the inlet velocity; (2) adopting that at the exit velocity; (3) adopting that at the arithmetic average of the inlet and exit velocity; (4) the product yield is the average of cases (1) and (2). In the first three cases, we figure out the flow hydrodynamics at first and then calculate the product yield. The parameters are the same as used in Section 3.4 except that the value of q is set at 4, and the results obtained by solving the varying SGV case are quoted as the accurate solutions.

The feed conversions are listed in Table 1. It shows that none of the results from four approximate methods is consistent exactly with those from the accurate method. Compared to the Approx. 1 and Approx. 2, the Approx. 3 and Approx. 4 produce more accurate results because they take both the inlet and exit into account. Additionally, the deviations are not the same for different reaction orders. For example, the gap between the conversion calculated from Approx. 3 and the accurate one is only 0.03% for the zero-order reaction while 3.39 and 5.08% for the first-order and second-order reactions, respectively. This can be explained by Fig. 8(a) that the reaction with a higher order tends to yield a more

Table 1
Comparison of feed conversion between the approximate and accurate methods for reactions with different orders (unit: wt.%)[a]

n	Approx. 1	Approx. 2	Approx. 3	Approx. 4	Accurate
0	10.42	8.65	9.43	9.53	9.40
1	98.69	48.61	72.34	73.65	68.95
2	99.45	84.66	94.72	92.06	89.64

[a] $q = 4$, $G_g = 5.22\,\mathrm{kg/(m^2\,s)}$, $G_s = 100\,\mathrm{kg/(m^2\,s)}$.

Table 2
Comparison between the results from the Approx. 3 and the accurate solution in FCC process[a]

	Accurate	Approx. 3	Absolute error
Conversion (wt.%)	79.12	88.49	+9.37
Gasoline yield (wt.%)	41.06	41.85	+0.79
Gas yield (wt.%)	34.24	42.37	+8.13
Coke yield (wt.%)	3.82	4.27	+0.45
Gasoline selectivity (%)	51.90	47.29	−4.61

[a] $G_g = 30.43\,kg/(m^2\,s)$, $G_s = 1200\,kg/(m^2\,s)$, $T = 550\,^{\circ}C$.

nonlinear distribution in gas velocity and result in a larger error in the average-velocity approximation method.

For those reactions with two or more products, the approximate methods may also lead to wrong estimation in product selectivity. As an example, the FCC process is simulated by adopting the model in [7] and the results are shown in Table 2. It can be seen that the adoption of Approx. 3 yields a 9.37 wt.% higher conversion than the accurate solution, while the selectivity of gasoline is underestimated by 4.61%. That means, the conversion and selectivity of a process under the varying SGV must be calculated by solving the transfer equations of mass, momentum and energy as well as the reaction kinetics instead of simply adopting the flow structure of the constant SGV case.

4. Conclusions

The simulation results above show that the SGV shapes the axial flow structure significantly in the downer reactor. The axial distribution of gas velocity, particle velocity, voidage, pressure and pressure gradient in the varying SGV case appears to have new features different from the constant SGV case, for example, the existence of the TAZ and the decreasing zone and the variation of gas density along the reactor length. Nevertheless, the conversion and selectivity are also significantly different between these cases. Because the varying SGV occurs frequently in the commercial plants, such a model is of interest for the application of downer reactor.

References

[1] Y.L. Yang, Y. Jin, Z.-Q. Yu, J.-X. Zhu, H.-T. Bi, Local slip behavior in the circulating fluidized bed, AIChE Symp. Ser. 89 (296) (1993) 81–90.
[2] C.-S. Cao, Y. Jin, Z.-Q. Yu, Z.-W. Wang, The gas–solids velocity profiles and slip phenomenon in a concurrent downflow circulating fluidized bed, in: A.A. Avidan (Ed.), Circulating Fluidized Bed Technology IV, AIChE, New York, 1994, pp. 406–413.
[3] D.-R. Bai, Y. Jin, Z.-Q. Yu, N.-J. Gan, Gas–solids flow patterns in a concurrent downflow fast fluidized bed (CDCFB), J. Chem. Ind. Eng. China (English Edition) 6 (2) (1991) 171–181.
[4] H. Zhang, J.-X. Zhu, M.A. Bergougnou, Flow development in a gas–solids downer fluidized bed, Can. J. Chem. Eng. 77 (1999) 194–198.
[5] P. Lehner, K.-E. Wirth, Characterization of the flow pattern in a downer reactor, Chem. Eng. Sci. 54 (1999) 5471–5483.
[6] J.-X. Zhu, Z.-Q. Yu, Y. Jin, J.R. Grace, A. Issangya, Cocurrent downflow circulating fluidized bed (downer) reactors—a state of the art review, Chem. Eng. Sci. 73 (1995) 662–677.
[7] R.-S. Deng, F. Wei, T.F. Liu, Y. Jin, Radial behaviors in riser and downer during FCC process, Chem. Eng. Process. 41 (3) (2002) 259–266.
[8] A. Shimizu, R. Echigo, S. Hasegawa, M. Hishida, Experimental study on the pressure drop and the entry length of the gas–solids suspension flow in a circular tube, Int. J. Multiphase Flow 4 (1978) 53–60.
[9] J.M. Kim, J.D. Seader, Pressure drop for cocurrent downflow of gas–solids suspensions, AIChE J. 29 (1983) 353.
[10] C.-M. Qi, Z.-Q. Yu, Y. Jin, D.-R. Bai, W.-H. Yao, Study on the gas–solids cocurrently downflow fluidization (I), J. Chem. Ind. Eng. China (Chinese Edition) (3) (1990) 273–280.
[11] C.-M. Qi, Y. Jin, Z.-Q. Yu, D.-R. Bai, X.-X. Zhong, Study on the gas–solids cocurrently downflow fluidization (II), J. Chem. Ind. Eng. China (Chinese Edition) (3) (1990) 281–290.
[12] Z. Wang, D. Bai, Y. Jin, Hydrodynamics of cocurrent downflow circulating fluidized bed (CDCFB), Powder Technol. 70 (1992) 271–275.
[13] J.S. Ball, J.X. Zhu, A preliminary study into the local solids fluxes in a downer reactor, Powder Technol. 114 (2001) 96–101.
[14] J.S. Ball, J.X. Zhu, A comparison of solids fluxes in a pair of downer and riser reactors, Chem. Eng. Technol. 23 (8) (2000) 701–705.
[15] J. Martin, E.E. Michaelides, in: Proceedings of the Third Multi-phase Flow and Heat Transfer Symposium, Miami Beach, 1983, p. 353.
[16] Y. Jin, Z.-Q. Yu, D.-R. Bai, Chem. React. Eng. Technol. (Chinese Version) (6) (1990) 17–23.